

Electron transmission through organized organic thin films studied by discrete initial electron kinetic energies

A. Haran¹, R. Naaman^{1,a}, G. Ashkenasy², A. Shanzer², T. Quast³, B. Winter³, and I.V. Hertel³

¹ Department of Chemical Physics, Weizmann Institute of Science, 76100 Rehovot, Israel

² Department of Organic Chemistry, Weizmann Institute of Science, 76100 Rehovot, Israel

³ Max-Born-Institut für Nichtlineare Optik und Kurzzeitspektroskopie, Postfach 1107, 12474 Berlin, Germany

Received 24 July 1998

Abstract. Synchrotron radiation (SR) pulses are used to eject electrons from a gold substrate covered with organized organic thin films (OOTF) in order to investigate their transmission probability through the OOTF as a function of the electron initial kinetic energy. By variation of the SR photon energy within a few eV above the Au-4*f* binding energy levels we controlled the initial kinetic energy of the substrate electrons. The observed oscillations in the transmission probability for porphyrin-based films as a function of the kinetic energy is argued to be due to effects of band structure above the vacuum level in the well-ordered molecular adsorbate. We also present valence photoemission spectra (PES) of different type OOTF and demonstrate how their coverage of the substrate affects the PES.

PACS. 79.60.Dp Adsorbed layers and thin films – 73.20.At Surface states, band structure, electron density of states – 73.61.Ph Polymers; organic compounds

1 Introduction

There is an increasing interest in measuring and understanding the conduction properties of supramolecular systems having nanoscale dimensions. The importance of the subject stems from its relevance to the possible design and production of molecular electronic devices [1]. It is also relevant to studies of charge transfer in biological systems, as well as for the understanding of high conductance through organic layers as measured with scanning tunneling microscopy (STM) [2]. In addition, these types of measurements may help to better model the interaction between electrons with sub-excitation energies and dielectric condensed matter [3].

The particular advantage in using organized organic thin films (OOTF) is the ability to deposit on surfaces organic molecules with well defined orientation and packing [4,5]. Due to their nature, it is possible to modify the film thickness in a controlled manner, layer after layer. In addition, the conformation of the long organic chains, necessary to form an OOTF, can also be altered. As we demonstrated recently, the electron transmission properties of OOTF depend on this property [6].

Porphyrins because of their photo- and electro-physical properties [7] are candidates in serving as light harvesting systems and in photo-electrical molecular electronic devices [8]. Therefore, the interaction between these molecules and electrons is of particular interest.

Electron transmission studies through OOTF can serve for determining the electronic properties of the organic molecules. Such processes can be investigated in several ways. A typical experiment of this type is electron photoemission through adsorbed molecular layers. Here the signal is the (angle and velocity resolved) transmitted electron flux as a function of incident photon energy, molecular film thickness, adsorbate and substrate types and temperature. A closely related experiment is low energy electron transmission (LEET) [9] where a monochromatic electron beam hits an adsorbed molecular layer from the vacuum side; the transmission is monitored *via* the current generated in the conducting substrate. The same experimental setup can be used to study reflection. Both transmission and reflection are studied as functions of the incident electron energy, substrate type and characteristics of the molecular layer.

Both methods do not provide a full state-to-state electron energy information. Usually, one is able to define either the initial energy and momentum of the electrons *before* they are transmitted through the OOTF (LEET), or to monitor the energy and momentum of the electrons *after* they were transmitted through the OOTF (photoemission studies).

In the present work we focus on a new experimental approach to investigate electron transmission (ET) through porphyrin-based thin films by generating electrons of well-defined “tunable” initial kinetic energies using synchrotron pulses. The energy of the electrons is

^a e-mail: cinaaman@wis.weizmann.ac.il

monitored following their transmission through the film. Hence, we demonstrate a novel experimental method in which the electron energy is well defined before entering the film and is fully analyzed following its transmission through the film. The present work is also a first demonstration of the electronic band structure above the vacuum level in metalloporphyrin monolayers.

In principle, resonances in electron transmission probabilities through atomic or molecular media, above the vacuum level, may be described either as diffraction of the electron wavefunction from the periodic structure of the film, or as transmission through resonance states, buried in the continuum, belonging to each molecule/atom. These vacuum resonances are actually the states of the anion, namely the electron-neutral species. These states, due to their large radius, interact with states located on neighboring species, hence forming a band structure [10]. These two descriptions appear to be of different origin on a superficial level, but actually describe the same phenomenon.

Electronic band structure in thin layers of dielectric materials has been observed earlier in layers of ordered rare gas and other simple molecular layers. The electron transmission [11], as well as the reflection [12] are strongly correlated with the band structure of the corresponding rare gas crystal. Similar behavior is expected for films of saturated hydrocarbon chains of various lengths [13,14]. The polymer thin films used in past studies were not ordered and it was therefore difficult to establish the effect of their organization on their electronic properties. In previous studies [15,16] we have demonstrated that such organic films are transparent to electrons of energy higher than 0.8 eV (above the vacuum energy), and the results were rationalized based on the electronic band structure in the OOTF [17].

The present paper first focuses on the photoemission spectra (PES) of two types of porphyrin-film systems (shown in Fig. 1a), dimethyl ester protoporphyrin IX iron chloride (DMPPFeCl) and tetraphenyl porphyrin iron chloride (TPPFeCl), and for comparison, on the self-assembled alkyl thiol monolayers of octadecyl mercaptane (OM) and hexyl mercaptane (HM) on gold, in order to demonstrate the changes in the PES of the substrate caused by the OOTF. In addition, we present data and discuss the electron transmission (ET) through porphyrin-based monolayer systems adsorbed on a gold substrate.

2 Experimental

2.1 Materials

The OOTF were prepared applying the self-assembly method. Silicon slides ($12 \times 13 \text{ mm}^2$) were coated with a 100 nm thick gold film prepared by vacuum evaporation. The gold films were treated with an ultraviolet ozone cleaner for 10 minutes to remove organic contaminants followed by immersion in ethanol for 20 minutes to eliminate gold oxide from the surface [18]. The slides were then immediately immersed in the adsorbate solution.

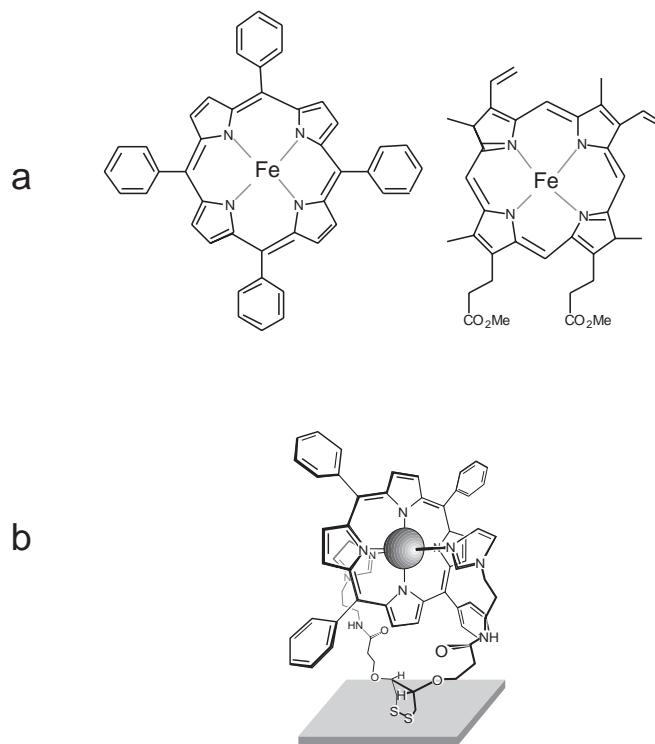


Fig. 1. (a) The structure of the two types of porphyrins used in the current study: TPPFe (left) and DMPPFe (right); (b) The postulated structure and orientation of TPPFe-bifunctional ligand complex bound to gold surface.

2.1.1 Preparation of alkyl thiol monolayers

Slides were immersed in 1 mM ethanol solution of octadecyl mercaptane [$\text{CH}_3(\text{CH}_2)_{17}\text{SH}$; OM] - (Merck, recrystallized) or 20 mM ethanol solution of hexyl mercaptane (HM) (Fluka) overnight. They were then taken out and washed with ethanol and chloroform.

2.1.2 Preparation of ironporphyrin monolayers

The synthesis of the bifunctional disulfide diimidazole ligand has been described elsewhere [19]. It has also been shown that the ironporphyrin molecule forms a complex with the bifunctional ligand [20]. Based on ^1H NMR data, it has been suggested that the two imidazolyl residues coordinate axially to the ironporphyrin while possessing perpendicular orientation to each other. Organized monolayers of the ironporphyrin-ligand complex have been prepared previously according to the procedure described below [19], and their characterization was carried out using ellipsometry, XPS and cyclic voltammetry.

Following the cleaning procedure outlined in the beginning of this section, the gold coated silicon slides were immersed in 2 mM chloroform solution of the ligand for 2–3 hours. They were then washed in chloroform and rinsed in ethanol for 15 minutes. Complexation was achieved by immersion of the slides in 5 mM chloroform

solution of TPPFeCl (Aldrich) or DMPPFeCl [21] for 8 minutes and rinsing in chloroform for additional 5 min. The thickness of alkyl thiol and ironporphyrin films was measured by an ellipsometer (Rudolph Research Auto-EL4) to verify monolayer quality (see Tab. 1). The two types of ironporphyrins are shown in Figure 1a. Figure 1b presents the postulated structure and orientation of the TPPFe – bifunctional ligand complex bound to gold surface.

2.2 Spectroscopy

2.2.1 Photoelectron Spectroscopy (PES)

The photoemission experiments were performed at the Berliner Elektronenspeicherring für Synchrotronstrahlung BESSY, Berlin. Synchrotron radiation (SR) was provided by the BESSY undulator (periodicity 70 mm) in the multi bunch mode at the TGM 6 monochromator. The photon energy range of this beam line is 12 to 120 eV. For the experiments presented here, the photon energy variation was at constant undulator gap (45 mm).

The experimental setup has been presented in greater detail elsewhere [22]. Briefly, the ultrahigh vacuum chamber is equipped with a hemispherical electron energy analyzer (EA 125; Omicron), combined retractable four-grid LEED/AES optics, a quadrupole mass spectrometer and rotatable sample manipulator. The base pressure was 2×10^{-10} torr. The undulator light was incident on the sample surface at 13° (focal size at the surface ca. 0.5×0.5 mm²). Photoelectrons were detected by the electron energy analyzer to within $\pm 8^\circ$ acceptance angle normal to the sample surface and the signal was recorded by counting electronics. For the current experiment the pass energy of the analyzer was set to 6 eV (constant energy mode) which corresponds to better than 150 meV kinetic energy resolution.

The PES were monitored at the beginning and at the end of each series of measurements and indicated the stability of the organic films. No indication for charging of the sample could be observed [23].

2.2.2 Electron transmission (ET) measurements

In previous studies, in order to investigate the transmission of low energy electrons through OOTF, we examined the secondary electrons emitted from the metal substrate [17]. These electrons are produced when UV radiation is applied on the surface and when some of the initially created photoelectrons undergo additional secondary processes, who lead to emission of low energy electrons with a wide energy distribution. In this case, it is possible to measure the energy of the electrons after they are transmitted through the OOTF, but their initial kinetic energy is only crudely defined.

The key to study transmission of electrons with discrete initial kinetic energies, rather than having to study the broad secondary electron distribution, is to eject photoelectrons from a well defined substrate state. In this

Table 1. Average film thickness calculated from ellipsometry results.

Film type	Average Thickness
Octadecyl mercaptane	17.1 ± 0.8 Å
DMPPFeCl	22.5 ± 0.3 Å
TPPFeCl	14 ± 3 Å

case, by varying the photon energy, the kinetic energies of the electrons are tuned to have any desired value. In the gold substrate, the two $4f$ states suit well to be the initial defined resonance and it is possible to produce highly monoenergetic electrons since the emission bands are very narrow and prominent (often used for energy calibration). Furthermore, the fact that these two lines are separated by 3.7 eV, allows to obtain two different initial kinetic energy values for each excitation photon energy. Since the Au- $4f_{5/2}$, $4f_{7/2}$ binding energies are 84.0 and 87.7 eV, respectively, the excitation photon energy has been varied between 95 and 105 eV in order to produce electrons with kinetic energies < 20 eV which cover the region of interest. In order to minimize discrimination effects of low-kinetic-energy electrons the sample was biased at -10 V. Proper intensity matching for different spectra and excitation energies has been performed to account for the variations of photon density as well as ring current changes.

3 Results and discussion

Figure 2 presents the valence photoemission spectra (PES) of the OM/Au monolayer system for different excitation photon energies as labeled in the figures. The energy scale is referenced to the gold substrate Fermi level E_F (which by definition corresponds to zero binding energy). For comparison we also show the PES of the short chain system HM (Fig. 2a). This comparison is useful for identifying the substrate contributions to the spectra. The spectra are all normalized to full scale. The reason for the differences in S/N when the excitation energy is varied are due to the monochromator properties; all the experiments have been performed without adjusting the undulator gap (see Sect. 2). Overall spectral features are in excellent agreement with the data reported in the literature for the same system [24,25]. Hence, for the following discussion the peak assignment has been directly adopted from these authors. Accordingly, features 1 and 2 in Figure 2 correspond to the C2*p* valence band and features 3 and 4 correspond to the C2*s* valence band. There is some contribution from the Au-5*d* levels near 3.5 and 6 eV (peaks a, b) which is seen to significantly vary as a function of photon energy. The small shoulder near E_F represents the Au *s* and *p* levels. In Figures 2a and 2b the PES of 6 and 18 carbon chains were both obtained at 55 eV excitation. For the short chain OOTF (Fig. 2a) only very low intensity C2*s* and C2*p* features are obtained. Hence, Figure 2a largely reflects the gold substrate PES [24]. In contrast, the long chain OOTF exhibit significant carbon contributions (Figs. 2b to 2d).

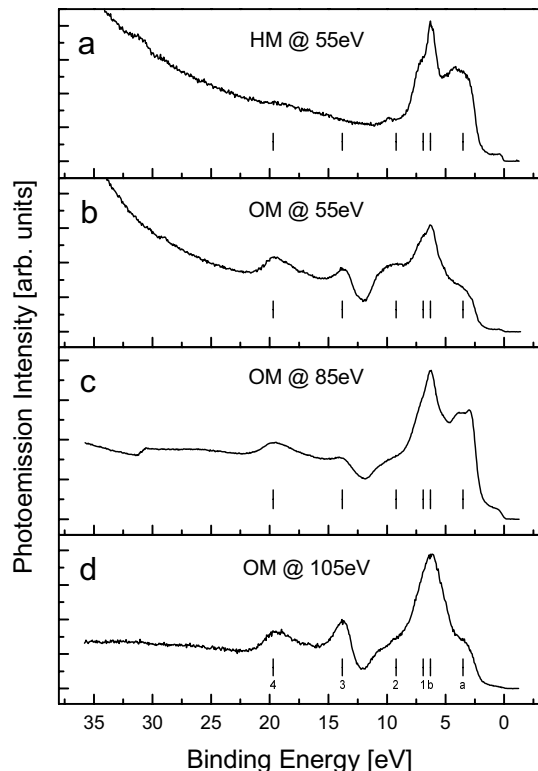


Fig. 2. Valence photoelectron spectra from alkylthiols monolayers on gold obtained for different excitation photon energies. (a) 1ML HM/Au (6 carbons alkyl chain) at 55 eV, (b) 1ML OM/Au (18 carbons alkyl chain) at 55 eV, (c) 1ML OM/Au at 85 eV and (d) 1ML OM/Au at 105 eV. Features 1 and 2 correspond to C2p level emission, features 3 and 4 correspond to the C2s levels, and labels a, b are the Au-5d contributions. The small hump at zero binding energy is the gold Fermi edge.

The OM PES at 85 eV is characterized by significantly increased Au-5d contributions because of the enhanced escape depth of electrons near 80 eV kinetic energies [26]. Other than that no appreciable changes are observed in the PES (Fig. 2c). At 105 eV the Au contribution decreases to a level even below the 55 eV case. This latter finding is in agreement with the results reported in references [24, 25] and reflects the significantly larger ionization cross section of the C2s and C2p levels than that of the Au-5d levels for excitation energies near the Au Cooper minimum. Useful for the purpose of this work is that with Figure 2 we have at hand a quick *in situ* level-referencing and thereby an immediate confirmation of the coverage of the films being investigated. The relationship between the PE features and the explicit geometrical structure of alkanethiols has been discussed in detail in reference [25]. Furthermore, given the above level assignments the assignment of the PES obtained for the two porphyrin films investigated here is straight forward.

Similarly to the thiols case (Fig. 2) we present in Figures 3 and 4 the corresponding PES data for a monolayer of DMPPFeCl/Au and TPPFeCl/Au (see Sect. 2.1) for the same photon energies, *i.e.* 55, 85, 105 eV. As ex-

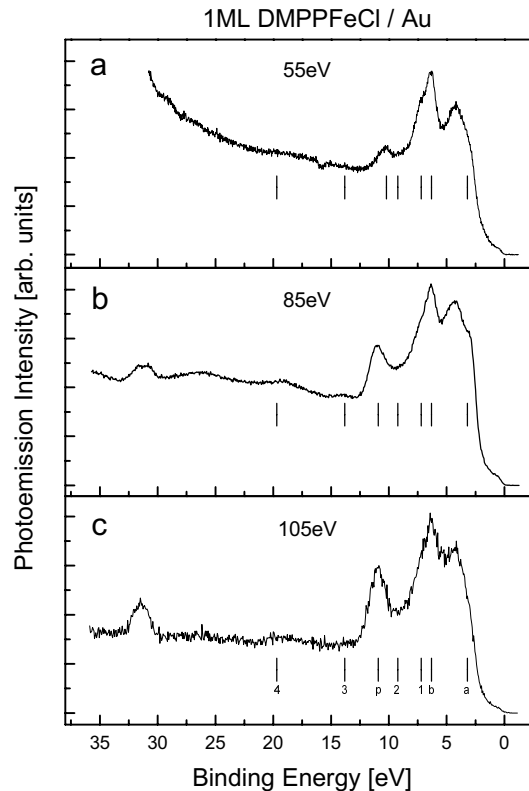


Fig. 3. Valence photoelectron spectra from ironporphyrin (DMPPFeCl) monolayers on gold obtained for 55 eV (a), 85 eV (b) and 105 eV (c) excitation photon energy, respectively. The peak labeling is the same as in Figure 2. Label p corresponds to the feature attributed to the porphyrin ring system.

pected the PES of both porphyrin systems do not show much of a photon energy dependence just like the short chain thiol data (Fig. 2a). The fact that the carbon features are somewhat more intense for the DMPPFeCl film as compared to the TPPFeCl system is due to possible contributions from trapping of solvent or even partial aggregation in the case of the DMPPFeCl. This is consistent with the somewhat larger film thickness measured by ellipsometry for this film (see Tab. 1).

Nonetheless, the trend of enhanced Au contributions at 85 eV and the decreased Au contributions at 105 eV is also observed. The peak positions are the same as for the thiols case, however, with one significant exception near 11 eV. This is best seen by comparing the DMPPFeCl and alkylthiols PE spectra both at 105 eV (Figs. 3c and 2d) as displayed in Figure 5. While there is a nearly monotonous intensity decrease from 7 eV to 12 eV for the latter case (Fig. 5b), which probably reflects some fingerprint character of the C2p region of alkylthiols, there appears an additional prominent feature centered at 11 eV binding energy for the porphyrin case (feature p in Figs. 3–5). Obviously, this new peak may be safely attributed to the presence of the porphyrin ring system. The above assignment is supported by comparison with the UPS data for 5 nm thick ZnTPP/Au (zinctetraphenylporphyrin)

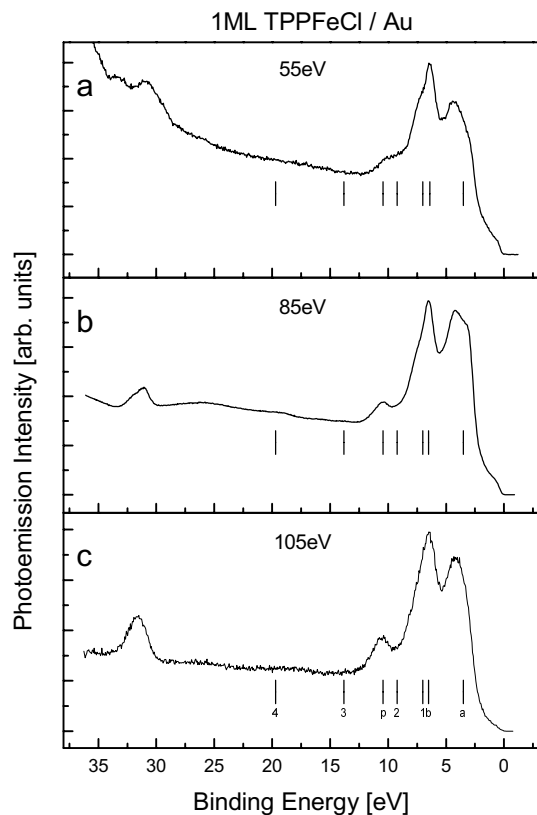


Fig. 4. Valence photoelectron spectra from ironporphyrin (TPPFeCl) monolayers on gold obtained for 55 eV (a), 85 eV (b) and 105 eV (c) excitation photon energy, respectively. The peak labeling is the same as in Figure 3.

reported in the literature [27] which, to our knowledge, is the only available PES data on (metallo)porphyrins. Although there is no perfect agreement in terms of relative intensities with our data (Figs. 3, 4), the fact that there do exist several strong peaks in the 7 to 12 eV region would be in favor of this assignment. Observed spectral differences are likely due to the different orientations of the porphyrin ring relative to the metal surface for the different porphyrin adsorbate systems. While in the present case the porphyrin ring is perpendicular to the substrate surface, held in position *via* two weak nitrogen bonds as part of the supporting carbon chains (see Sect. 2.1 and Fig. 1b), adsorption of porphyrin directly on the surface would most likely yield in the nearly substrate-parallel configuration. It is also noted that the PES of thick ZnTPP film exhibits strong ring-related features – ascribed to the nearly degenerate two *p* orbitals delocalized over the central macrocycle – which appear right in the Au-5*d* region.

The effect of the band structure above the vacuum level in porphyrin on the electron transmission probability is studied using electrons of different initial kinetic energies and is documented in Figure 6. Shown are the background subtracted Au-4*f*_{5/2}, 4*f*_{7/2} states (87.7 and 84.0 eV binding energy, respectively) as a function of three different excitation photon energies, 95, 103, 105 eV from 1ML TPPFeCl/Au. The displayed individual sec-

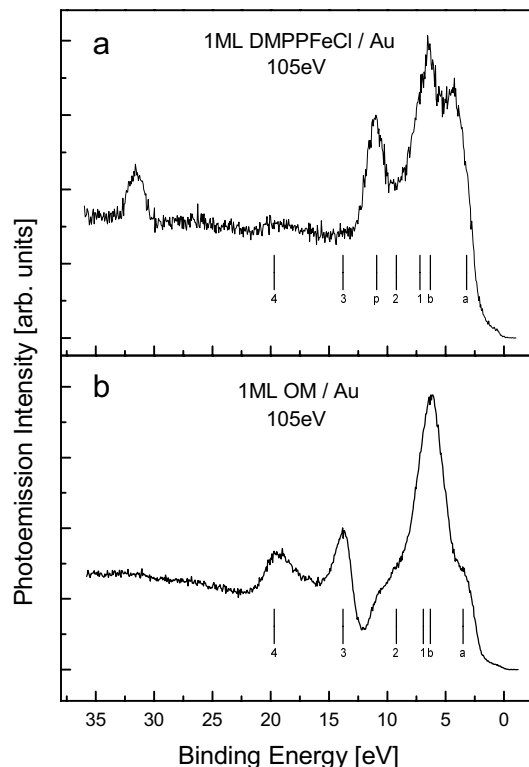


Fig. 5. Comparison of the PES for 1ML DMPPFeCl/Au and 1ML alkylthiol (OM)/Au both obtained at 105 eV photon energy.

tions of the PES are matched such that the respective 4*f* peaks are vertically aligned. The energy values given here refer to the true initial electron kinetic energies (*i.e.* $E_k = h\nu - \text{WF-BE}$) [28]. There is a pronounced change observed in the (Au-4*f*_{5/2}) / (Au-4*f*_{7/2}) peak ratio which is roughly 1.4 for 95 eV, 1.0 for 103 eV and 0.6 for 105 eV excitation energies. This relative intensity variation is argued to be due to the changing electron transmission probability through the porphyrin film as the initial electron kinetic energy varies. If there were no band structure effects involved one would expect a constant 4*f* peak ratio near 0.7. Indeed, monotonic variation of the peak ratio as a function of photon energy is expected and was reported in the literature [29,30]. However, these significant fluctuations in the branching ratio at such narrow energy range indicate that the observed effect is due to the adsorbed layer.

For a more quantitative analysis of the experimental data we plot in Figure 7 all measured Au-4*f* peaks on a common kinetic energy scale. Intensities have been corrected for the actual ring beam current and the monochromator function as well as for the degeneracy difference between the 4*f*_{5/2} and 4*f*_{7/2} peaks. The dashed curve is an attempt to visually emphasize the oscillations of the Au-4*f* peaks intensities induced by the band structure of the film.

The decrease in the transmission observed at low energies (below 6 eV) is consistent with our previous results,

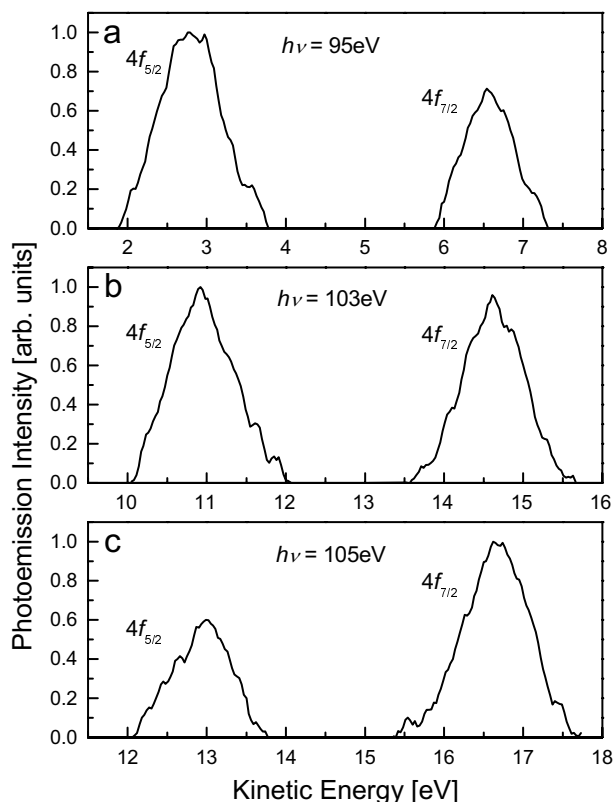


Fig. 6. Au- $4f_{5/2}$ and Au- $4f_{7/2}$ photoemission from 1ML TPPFeCl/Au (after subtracting the secondary emission background) for 95 eV (a), 103 eV (b) and 105 eV (c) excitation photon energy, respectively. Shown are the PES as a function of the effective kinetic energies of the electrons. The changing intensity ratio of the two levels, $4f_{5/2}$ to $4f_{7/2}$, reflects the varying probability for electron transmission through OOTF as a function of the electrons initial kinetic energy.

where the transmission probability of electrons transmitted through films of cadmium arachidate was shown to decrease for kinetic energies above ca. 1.0 eV [17]. At present, there is no theoretical description available for the band structure, that can be compared to the data presented and we refrain from discussing these results quantitatively. However, strong electron transmission variations have been calculated for a 4-argon-layers model system, in accord with the experiment [17]. Certainly, more work, both experimentally and theoretically, is required in order to explain the above results. In particular a higher resolution study is required, in which the kinetic energy of the electrons excited from the Au- $4f$ state will be tuned with small energy increments and the ballistic transmission probability will be measured. Clearly, having available initial electrons of well-defined energy and momentum as demonstrated here is a very promising tool to investigate the ET in much more detail.

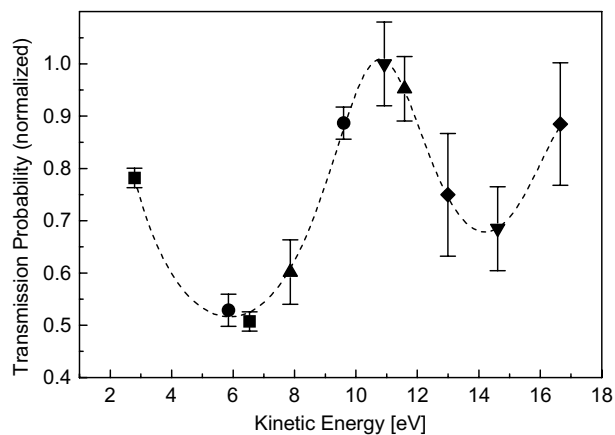


Fig. 7. Plot of the measured Au- $4f_{5/2,7/2}$ (relative) peak intensities as a function of the actual electrons kinetic energies (as due to different excitation energies: (■) 95 eV, (●) 98 eV, (▲) 100 eV, (▼) 103 eV and (◆) 105 eV) obtained for 1ML TPPFeCl/Au. The $f_{5/2}$ to $f_{7/2}$ relative intensities (at a given photon energy) have been corrected for the degeneracy by the factor 7/5. The fit serves to guide the eye. The observed oscillations reflect the changing probability for electron transmission through OOTF as a function of the electrons initial kinetic energy.

4 Conclusions

The study described here is the first attempt to carry out a fully energy resolved electron transmission experiment through OOTF. By applying a SR tunable source and utilizing a narrow emission resonance of the substrate we were able to obtain the ballistic transmission probability of electrons through organic layers as a function of the energy of the electrons. Applying this scheme we were able to demonstrate the electronic band-like structure above the vacuum level in a monolayer of a porphyrin.

R.N. and A.H. acknowledge the partial support by the Israel Science Foundation, the G.M.J. Schmidt Minerva Center for Supramolecular Architectures, as well as support through the EU-TMR Program. The two groups from the Weizmann Institute acknowledge the partial support by the Minerva Foundation. The MBI group acknowledges financial support by the Bundesministerium für Bildung, Wissenschaft, Forschung und Technologie under Contract No. 05 650BMA 6.

References

1. F.L. Carter (Marcel Dekker Inc., New York, 1987), Vol. 2; J.M. Lehn, *Angew. Chem.* **100**, 89 (1988); *Molecular and Biomolecular Electronics*, edited by R.R. Birge (American Chemical Society, Washington D.C., 1994); A. Aviram, M.A. Ratner, *Chem. Phys. Lett.* **29**, 277-283 (1974).
2. A. Ikai, *Surface Sci. Rep.* **26**, (1996); J.A. DeRose, R.M. Leblanc, *ibid.* **22**, (1995) and references therein.
3. U. Fano, J.A. Stephens, *Phys. Rev. B.* **34**, 438 (1986).

4. M. Schreck, D. Schmeisser, W. Gopel, H. Schier, H.U. Habermeier, S. Roth, L. Dulog, *Thin Solid Films* **175**, 95 (1989).
5. A. Ulman, *Introduction to Ultrathin Organic Films* (Academic Press, 1991) and references therein.
6. A. Haran, D.H. Waldeck, R. Naaman, E. Moons, D. Cahen, *Science* **263**, 948 (1994).
7. For example: K. Uosaki, T. Kondo, X-Q. Zhang, M. Yanagida, *J. Amer. Chem. Soc.* **119**, 8367 (1997); T.J. Savenije, E. Moons, G.K. Boschloo, A. Goossens, T.J. Schaafsma, *Phys. Rev. B* **55**, 9685 (1997).
8. For example: A. Hagfeldt, M. Gratzel, *Chem. Rev.* **95** (1995) 49; G. Steinberg-Yfrach, P.A. Liddell, H. Su-Chun, A.L. Moore, D. Gust, T.A. Moore, *Nature* **385**, 239 (1997).
9. L. Sanche, *Scanning Microscopy* **9**, 619 (1995).
10. R. Naaman, A. Haran, A. Nitzan, D. Evans, M. Galperin, *J. Phys. Chem. B*, **102**, 3658 (1998).
11. G. Bader, G. Perluzzo, L.G. Caron, L. Sanche, *Phys. Rev. B* **30**, 78 (1984); G. Perluzzo, G. Bader, L.G. Caron, L. Sanche, *Phys. Rev. Lett.* **55**, 545 (1985).
12. M. Michaud, L. Sanche, C. Gaubert, R. Baudoing, *Surf. Sci.* **205**, 447 (1988); T. Goulet, J.-M. Jung, M. Michaud, J.-P. Jay-Gerin, L. Sanche, *Phys. Rev. B* **50**, 5101 (1994).
13. L.G. Caron, G. Perluzzo, G. Bader, L. Sanche, *Phys. Rev. B* **33**, 3027 (1986).
14. T. Maeda, K. Miyano, K. Sugita, N. Ueno, *Thin Solid Films* **179**, 327 (1989); N. Ueno, H. Nakahara, K. Sugita, K. Fukuda, *ibid.* **179**, 161 (1989); N. Ueno, K. Sugita, *Phys. Rev. B* **42**, 1659 (1990).
15. A. Kadyshkevitch, R. Naaman, *Phys. Rev. Lett.* **74**, 3443 (1995).
16. A. Kadyshkevitch, R. Naaman, *Thin Solid Films* **288**, 139 (1996).
17. A. Haran, A. Kadyshkevitch, H. Cohen, R. Naaman, D. Evans, T. Seideman, A. Nitzan, *Chem. Phys. Lett.* **268**, 475 (1997).
18. H. Ron, I. Rubinstein, *Langmuir* **10**, 4566 (1994).
19. G. Ashkenasy, G. Kalyuzhny, J. Libman, I. Rubinstein, A. Shanzer, *Angew. Chem. Int. Ed. Engl.* (1999) in press.
20. F.A. Walker, M.-W. Lo, M.T. Ree, *J. Amer. Chem. Soc.* **98**, 5552 (1976).
21. Synthesis of DMPPFeCl is described in: L.H. Guo, G. Mclendon, H. Razafitrimo, Y. Gao, *J. Mater. Chem.* **6**, 369 (1996).
22. T. Quast, R. Bellmann, B. Winter, J. Gatzke, I.V. Hertel, *J. Appl. Phys.* **83**, 1642 (1998).
23. In former studies we established that thin organic films (up to about 2.5 nm) which are covalently bound to the metal substrate do not tend to be charged, while physisorbed films of similar thickness are charged. (A. Haran, H. Cohen, R. Naaman, to be published).
24. A.-S. Duwez, J. Riga, J. Ghijsen, J.J. Pireaux, J.J. Verbist, J. Delhalle, *J. Electron Spectrosc. Relat. Phenom.* **76**, 523 (1995).
25. A.-S. Duwez, S. Di Paolo, J. Ghijsen, J. Riga, M. Deleuze, J. Delhalle, *J. Phys. Chem.* **101**, 884 (1997).
26. S. Hüfner, *Photoelectron Spectroscopy – Principles and Applications*, Springer Series in Solid-State Sciences, **82** (1995).
27. H. Ishii, S. Narioka, D. Yoshimura, M. Sei, Y. Ouchi, S. Hasegawa, T. Miyazaki, Y. Harima, K. Yamashita, K. Seki, *J. Electron Spectrosc. Relat. Phenom.* **76**, 559 (1995).
28. Here WF is the Au-polycrystalline workfunction (5.0 eV), $h\nu$ denotes the photon excitation energy and BE is the Au-4f binding energy.
29. K. Gürtel, K.H. Tan, G.M. Bancroft, P.R. Norton, *Phys. Rev. B* **35**, 6024 (1987).
30. S. Varma, Y.J. Kime, D. LaGraffe, P.A. Dowben, M. Onellion, J.L. Erskine, *J. Chem. Phys.* **93**, 2819 (1990).